Title

Morphometric Analysis and Linear Measurements of the Scala Tympani and Implications in Cochlear Implant Electrodes.

Journal

The American journal of otology, 44(5)

Authors

Fujiwara, Rance
Ishiyama, Gail
Ishiyama, Akira
et al.

Publication Date

2023-06-01

DOI

10.1097/MAO.0000000000003848

Peer reviewed

HHS Public Access

Author manuscript

Otol Neurotol. Author manuscript; available in PMC 2024 June 01.

Published in final edited form as:

Otol Neurotol. 2023 June 01; 44(5): e343–e349. doi:10.1097/MAO.0000000000003848.

Morphometric analysis and linear measurements of the scala tympani and implications in cochlear implant electrodes

Rance J.T. Fujiwara, MD MBA[a], **Gail Ishiyama, MD**[b], **Ivan A. Lopez, PhD**[a], **Akira Ishiyama, MD**[a]

[a]David Geffen School of Medicine at UCLA, Department of Head and Neck Surgery, Los Angeles 90095

[b]David Geffen School of Medicine at UCLA, Department of Neurology, Los Angeles 90095

Abstract

Hypothesis: The objective of this study was to perform detailed height and cross-sectional area measurements of the scala tympani in histologic sections of non-diseased human temporal bones and correlate them with cochlear implant electrode dimensions.

Background: Prior investigations in scala tympani dimensions have utilized micro-CT or casting modalities, which cannot be correlated directly with microanatomy visible on histologic specimens.

Methods: 3-D reconstructions of 10 archival human temporal bone specimens with no history of middle or inner ear disease were generated using H&E histopathologic slides. At 90° intervals, the heights of the scala tympani at lateral wall, mid-scala, and perimodiolar locations were measured, along with cross-sectional area.

Results: The vertical height of the scala tympani at its lateral wall significantly decreased from 1.28 mm to 0.88 mm from 0° to 180°, and the perimodiolar height decreased from 1.20 to 0.85 mm. The cross-sectional area decreased from 2.29 (sd 0.60) mm^2 to 1.38 (sd 0.13) mm^2 from 0° to 180° (p=0.001). After 360°, the scala tympani shape transitioned from an ovoid to triangular shape, corresponding with a significantly decreased lateral height relative to perimodiolar height. Wide variability was observed among the cochlear implant electrode sizes relative to scala tympani measurements

Conclusion: The present study is the first to conduct detailed measurements of heights and cross-sectional area of the scala tympani and the first to statistically characterize the change in

Corresponding author: Akira Ishiyama, MD, 10833 Le Conte Ave, 62-132 CHS, Los Angeles, CA 90095, aishiyama@mednet.ucla.edu.

Author Contributions:

Rance J.T. Fujiwara: Conceptualization, Methodology, Software, Validation, Formal analysis, Investigation, Data curation, Writing – Original Draft, Visualization

Gail Ishiyama: Methodology, Investigation, Validation, Writing – Review & Editing, Supervision, Visualization

Ivan A. Lopez: Validation, Resources, Writing – Review & Editing, Supervision, Project administration, Funding acquisition

Akira Ishiyama: Conceptualization, Methodology, Validation, Resources, Writing – Review & Editing, Visualization, Supervision, Project administration, Funding acquisition

Conflicts of interest: The authors have no conflicts of interest to disclose.

its shape after the basal turn. These measurements have important implications in understanding locations of intracochlear trauma during insertion and electrode design.

Keywords

scala tympani; temporal bone; cochlear implant; electrode design; 3-D reconstruction

Introduction

Patients with moderate to profound bilateral sensorineural hearing loss, who demonstrate inadequate benefit from hearing amplification, may benefit from cochlear implantation, which has now become the standard of care and has been shown to improve global cognitive function, quality of life scores, and other long-term benefits.[1-3] Recently, efforts have focused on performing implantation as atraumatically as possible, for residual hearing preservation and minimalization of triggers of fibrosis.[4,5] Immediate or delayed intracochlear pathology, such as translocation across the basilar membrane, through the organ of Corti, or lateral wall damage may trigger fibrosis and osteneogenesis, resulting in nonoptimal audiologic outcomes postoperatively.[6-8]

Two recent studies showed that translocations across the basilar membrane were most likely to occur at angular insertion depths near either 180° or 400°.[6,9] To date, several studies have been conducted looking at cochlear microanatomy and dimensions of the scala tympani (ST).[9-15] Limited work has provided detailed morphometric analyses of the ST that explain why these areas are susceptible to electrode translocation, and few have compared such measurements to that of current cochlear implant electrodes. The most extensive analysis was performed by Avci *et al.*, who utilized micro-CT in non-implanted human temporal bone specimens to record three different ST vertical heights along the length of the cochlea.[11] Detailed studies utilizing histologic human temporal bone specimens, however, have not been performed.

The purpose of this study is three-fold. First, as previously demonstrated, we seek to perform 3-D reconstruction of histologic sections of human temporal bone specimens, which has not been performed in the current literature for the purposes of scala tympani morphometric analysis.[16] Second, the vertical height and cross-sectional area of the scala tympani are measured at 90° intervals using the round window as the 0° reference point, as established by Verbist *et al.*[17] Vertical height measurements are obtained at three different horizontal positions in order to better approximate the designed lateral and perimodiolar positions of cochlear implant electrodes. Third, the cross-sectional area and height of current electrodes are compared to scala tympani measurements.

Materials and methods

Human temporal bones

A total of 10 human temporal bone (HTB) specimens (5 right, 5 left) from 9 subjects (5 male, 4 female) with no history of middle or inner ear surgery, no audiological diseases which would affect the labyrinthine structures such as Meniere's disease or labyrinthitis

ossificans, and no history of cochlear implantation, were included in this study. Age at death ranged from 15 to 82 years old. This study was approved by the UCLA Institutional Review Board (IRB protocol #10-001449). All methods used in this analysis are in accordance with NIH and IRB guidelines and regulations. The temporal bone donors were part of a National Institute of Health funded National Temporal Bone Laboratory at UCLA through the National Institute on Deafness and Other Communication Disorders. Each medical record from patients who have donated their temporal bones was reviewed and maintained within a secured electronic database.

HTB processing

The temporal bones were removed postmortem and processed as has previously been described.[16,18] Briefly, they were placed in 10% neutral buffered formalin for 3 weeks, decalcified in ethylenediaminetetraacetic acid until shown by x-ray to be free of calcium. Embedding was done in increasingly concentrated celloidin to allow for complete penetration. The temporal bones were then exposed to fumes to chloroform for 4 weeks (in a desiccator) to allow for polymerization of the celloidin. The celloidin block was then cut into 20 micron sections, of which every tenth section was mounted and stained with hematoxylin and eosin (H&E).

3-Dimensional reconstruction of the cochlea

The serial images (27-38 slides) of 10 HTB specimen were examined under light microscopy under a 10x objective (Leica DMi8) and captured using a digital camera (Leica DFC 7000T) within the Leica Application Suite X (LAS X, Leica Microsystems, Wetzlar, Germany) software. The images were imported into the Fiji (Fiji Is Just ImageJ) software program; automatic alignment was performed using the TrakEM2 plugin and verified manually using fiduciary landmarks, including the modiolus, internal auditory canal, and semicircular canals. The aligned stacks were then uploaded onto Amira (version 2022.1) to generate 3-D reconstruction. Dimensions in the x and y axes of each voxel within Amira were input based on pixel and linear dimensions provided by LAS X software; to account for the nine unstained sections between each H&E section, the voxel dimension in the z axis was set at 200 μm (20 μm-thick sections multiplied by 10 sections). For each specimen, the entire cochlea and ST were segmented using the ‘Segmentation’ tool within Amira to generate surfaces of each 3-D reconstruction (Figure 1). The ‘Smooth Surface’ module was then used to smooth the surface of each reconstruction.

Linear height and cross-sectional measurements of the ST

The standard Cochlear view and coordinate system established by a 2010 consensus panel was then utilized for all measurements, as has previously been performed.[16,17] Briefly, a line from the center of the round window and through the modiolus and terminating at the lateral wall of the basal turn corresponds with the 0° and 180° reference points (y-axis), with the x-axis perpendicular and establishing the 90° and 270° reference points. The line from the helicotrema through the intersection of the x- and y-axes represents the z-axis. At 90° intervals of angular distance from 0° (round window) to 810°, cross-sections of the ST were generated with the ‘Surface Cross Section’ tool. The height of the ST was measured at 3 different points every 90°: the height at the horizontal center of the lateral and modiolar

walls, the height 0.2mm from the lateral wall, and the height 0.2mm from the modiolar wall, as has previously been performed in the literature.[11] The cross-sectional area of the ST was calculated every 90° using the 'Patches' mode of the 'Surface Area Volume' module (Figure 2).

Cochlear implant electrode dimensions

The length of ten cochlear implant electrodes, in addition to their individual heights and widths at their apex and base, were obtained from publicly available manufacturer data from three major cochlear implant electrode companies as well as current literature. [19-21] This included the Cochlear (Cochlear Limited, Sydney, Australia) Slim Straight (CI622), Slim Modiolar (CI632), and Hybrid L24 electrodes; the MED-EL (Innsbruck, Austria) FLEX Soft, FLEX 24, and FLEX 28 electrodes; and the Advanced Bionic (Advanced Bionics, LLC, Valencia, California, USA) 1J, Helix, Midscala, and Slim J electrodes. The estimated angular depth of insertion, equivalent to the angular depth at which the electrode apex would be positioned with full insertion, was determined by a review by Dhanasingh and Jolly in 2017.[19] Detailed manufacturing information regarding the linear length at which each stimulating electrode was positioned, as well as the height and width at each stimulating electrode position, was obtained directly from Cochlear Limited for the Slim Modiolar and Slim Straight electrodes. Identical information for the MED-EL FLEX 28 was gathered from a review by Dhanasingh in 2021.[22]

The cross-sectional area of each electrode at its apex and base was calculated using the area formula for an ellipse πab, where a is the major radius (half of implant width) and b is the minor radius (half of implant height). The percentage of occupied ST was calculated by dividing each electrode apex's cross-sectional area by the ST cross-sectional area at full insertion. The area of each electrode's base was calculated as a percentage of the round window cross-sectional area, which was determined from a previous study by Shakeel *et al.*[23]

Detailed electrode dimension calculations for CI632, CI622, and FLEX28

Finally, with the detailed specifications obtained for the Cochlear Americas Slim Modiolar and Slim Straight electrodes, and for the MED-EL FLEX 28, we performed two calculations every 90° assuming full electrode insertion: first, the percentage of ST cross-sectional area occupied (as described above); and second, the maximal potential distance from the electrode to the basilar membrane. The angular position of each stimulating electrode for the CI632 and CI22 electrodes was estimated utilizing previously calculated outer and inner cochlear wall linear distances.[16] The maximal potential distance from electrode to basilar membrane was estimated using the height specified for each electrode and the ST heights calculated above.

All statistical analysis was performed on Stata 14.2 (StataCorp, College Station, TX). Means and standard deviations were calculated for each height and cross-sectional area measurement every 90 degrees. Two-sided paired student's t-test was utilized to compare overall means of the lateral, central, and perimodiolar heights. To determine statistically significant changes between each 90° interval, one-way repeated measures ANOVA was

conducted. A *post hoc* analysis using the Bonferroni correction was performed to determine statistically significant changes in the means of these measurements at each 90° interval while accounting for the problem of multiple comparisons.

Results

Scala tympani vertical height

Analysis of the 3-D reconstructions of the 10 temporal bone specimens showed notable variability in the ST. Table 1 details the means and standard deviations of the central height, lateral height, and perimodiolar height at 90° intervals. The central height was significantly greater in length than both the lateral and perimodiolar measurements ($p<0.001$). Generally, the ST assumes an ovoid shape over its basal turn, and over the course of the middle turn develops a triangular shape with its perimodiolar height greater than its lateral height. The transition from 360° to 450° appeared to be the transition point of the shape change. At less than 360°, the lateral height had a mean of 0.92 mm (sd 0.25), and the perimodiolar height was 0.99 mm (sd 0.29) ($p=0.09$), as expected in an ovoid shape. However, at >360°, the perimodiolar height (mean 0.71mm, sd 0.23) was significantly greater than the lateral height (0.53 mm, sd = 0.21) ($p<0.001$), consistent with the change to a pyramidal or triangular shape in the scala tympani beyond the first cochlear turn.

The largest interval decrease in height for all three measurements occurred over the first half of the basal turn. For the central height, there was a significant decrease from 0° to 90° from 1.79 mm (sd 0.38) to 1.39 mm (sd 0.14) ($p=0.002$) on ANOVA testing, and again from 90° to 180° (1.09 mm [sd 0.15], $p=0.001$). The lateral height significantly decreased from 1.28 mm (sd 0.25) to 0.85 mm (sd 0.10) ($p=0.002$) over the first 90°. While no change in perimodiolar height from 0° to 90° was observed, there was a significant decrease from 90° to 180°, from 1.21 mm (sd 0.35) to 0.85 mm (sd 0.15) ($p=0.001$).

In all three height measurements, a relative plateau was also observed from roughly 180° to 450°. After 450°, the central, lateral, and perimodiolar heights each had steady, slow decreases in their magnitudes. There were no statistically significant decreases over 90° increments from 450° to 810°.

Scala tympani cross-sectional area measurements

The measurements of the ST cross-sectional area for all ten specimens are depicted in Figure 3. The largest variability in area measurements occurred over the first half of the basal turn. From 0° to 90°, the ST area significantly decreased from 2.29 mm^2 (sd 0.60) to 1.95 mm^2 (sd 0.59) ($p=0.002$). The ST area also significantly decreased from 90° to 180° (1.38 mm^2 [sd 0.13], $p=0.001$).

Cochlear implant electrodes

Using available manufacturing data and prior studies on the angular depth of insertion of individual electrodes,[19] the percentage of ST cross-sectional area occupied by each electrode's apex was calculated. The calculations are detailed in Figure 4. Among the perimodiolar electrodes, the CI632 occupies 12.51% (sd 2.78%), compared to 22.34% (sd

4.97%) and 32.16% (sd 7.16%) for the Midscala and Helix, respectively. Among lateral wall electrodes, the CI622 occupies 7.82% (sd 1.74%), FLEX24 13.40% (sd 2.98%), and SlimJ 12.78% (sd 2.84%).

Detailed electrode dimensions for CI632, CI622, and FLEX28

Finally, detailed electrode dimensions at each stimulating electrode location were obtained for the CI632, CI622, and FLEX28 electrodes; at 90° intervals, the percentage of occupied cross-sectional area as well as the maximal potential distance from the basilar membrane to the electrode were determined. For the perimodiolar CI632, the electrode occupied a mean ST cross-sectional area of 11.62% (sd 3.70, range 8.71–13.57%), and the vertical distance was 0.28 mm (sd 0.13, range 0.21–0.38 mm) from the basilar membrane. In contrast, the lateral wall CI622 occupied mean 10.67% (sd 3.24, range 9.38-12.3%), with vertical distance 0.25 mm (sd 0.11, range 0.19-0.39 mm); the FLEX28 occupied 21.94% (sd 7.90, range 15.76-28.76%), with distance from basilar membrane 0.15 mm (sd 0.10, range 0.05-0.13). The interval measurement averages are depicted in Figure 5.

Discussion

In the present study, we have detailed the vertical heights and cross-sectional area of the scala tympani using 3-D reconstruction of histologic sections in normal human temporal bone specimens without pathology and without a history of implantation. We compared these measurements to the current catalogue of cochlear implant electrode arrays and determined notable variability among currently utilized electrodes. Measurements were made using the coordinate system established by Verbist *et al.* in 2010.[17]

The ST vertical height in the central portion, lateral wall, and perimodiolar region all showed a statistically significant decrease over the first 180° of the basal turn of the cochlea as well as a steady decline in heights after 450°. Most prior studies have found an inverse correlation between distance from round window and ST height and area, though often do not account for the changing shape of the ST cross-section, measure along different horizontal ST positions, or perform detailed statistical analysis.[10,12-14] A recent study by Avci *et al.* utilized 3-D reconstruction of micro-CT images to measure scala tympani height by lateral wall, central, and peri-modiolar dimensions.[11] Despite using similar methodology, several differences were observed. First, the authors did not observe a decrease in the lateral or peri-modiolar heights over the first 180°, while we have identified a statistically significant decrease over the first half-turn. Of note, several other temporal bone studies found decreases in ST height over the first half-turn, though only measured along central horizontal locations.[12,13] Second, while Avci *et al.* also found a significant decrease in the lateral wall height after 450°, from 0.86 mm to 0.35 mm from the round window to the end of the second turn, they found minimal change in the height of the perimodiolar scala tympani, decreasing from 0.82 mm to 0.72 mm from the round window to the end of the second turn. Again, the present study on human temporal bone specimens demonstrated significant decreases in height in all three regions of the scala tympani within 180° from the round window. Furthermore, we have statistically characterized the transition point in the cross-sectional contour of the scala tympani from 360° to 450°, from an ovoid shape to a

triangular shape with the perimodiolar region the tallest region. Avci *et al.* also comment on a similar change in shape without metric analysis. Finally, Avci *et al.* removed perilymph fluid in order to conduct CT studies and noted that the apical area could not be evaluated as a result, which may have affected the ST morphometry and resultant measurements relative to histologic temporal bone measurements.

The cross-sectional area also significantly decreased from 2.29 mm^2 to 1.38 mm^2 from 0° to 180°. Avci *et al.* similarly found a maximum cross-sectional area of 2.3 mm^2 within the first 20° of the basal turn;[11] a subsequent drop in area was also observed over the first 180°, though no statistical analysis or comment was made regarding this finding. Hatsushika *et al.* observed an initial rapid decrease in ST cross-sectional area over the first 1.5 mm from the round window, as well as a decrease from 2.25 mm^2 to 1.2 mm^2 at 14 mm from the round window, which is roughly equivalent to 180° in angular distance.[12,16]

The findings above have significant implications in cochlear implantation and the location of electrode translocation. Ishiyama *et al.* examined 13 HTB specimens with translocation injury implanted with first-generation cochlear implant electrodes.[6] Translocation injuries tended to occur near 180° of angular insertion, with a mean of 186.36±51.62°; sites of translocation associated with lateral wall injury or scala media disruption were associated with a much greater degree of fibrosis and osteoneogenesis, which corresponded with loss of spiral ganglion neurons and poorer speech performance. Utilizing either intraoperative cone-beam CT or postoperative CBCT or traditional CT imaging, Morrel *et al.* in 2020 studied 177 implanted ears, reporting 39 exhibited translocations.[9] Higher angular insertion depths were correlated with increased rates of translocation; the median angular depth of translocation was 381° and followed a bimodal distribution, with most occurring around 400° and a smaller subset around 200°. The localized angular distance of translocation at 180° corresponds with the most significant decrease in both ST height and cross-sectional area demonstrated in the present study, suggesting that the precipitous decrease in the size of the scala tympani at this location places this area at increased risk for translocation. The localization of translocation injuries at 400° corresponds with the location at which the scala tympani assumes a more triangular shape with a decrease in lateral relative to perimodiolar heights from 360° to 450°. The change in conformation of the ST may affect the trajectory of a lateral wall electrode upon insertion and, coupled with the decreasing (albeit not statistically significant) ST size, may displace the electrode through the basilar membrane or osseous spiral lamina and predispose to significant lateral wall injury at the deeper angular insertions of the lateral wall electrode. Of note, Morrel *et al.* also commented that 8 of 10 insertions greater than 650° had translocations; we observed a precipitous drop from 630° to 720° particularly in the lateral ST height, which corresponds with this finding.

The notable variability in electrode diameter may have important implications in audiological outcomes. An additional consideration is the drop in the lateral wall height beyond 360° which may also indicate areas at risk of translocation injury with deeper angular insertion of the lateral wall electrode compared with the perimodiolar electrode. Larger electrodes may be displaced from the lateral wall, abut the basilar membrane at earlier insertion depths, or require increased insertional force, and as such may be more likely to incite inflammatory responses via lateral wall injury or abutment or displacement of

the basilar membrane.[24] Even in the absence of translocation, fibrosis and osteoneogenesis may occur, with new bone formation increasing over time and correlated with worse postoperative audiologic measures.[25] Increasing amounts of new bone formation have been positively correlated with degree of intracochlear insertional trauma, which may then result in worsened postoperative audiologic outcomes.[6,26] As such, additional work needs to be performed in the importance of electrode dimensions in the prediction of intracochlear insertional trauma.

Several limitations exist to the present study. First, the study is limited to a small sample size of ten human temporal bone specimens. Second, our measurement of "maximal potential distance" is a rough estimate of the true distance from electrode to basilar membrane; in non-implanted specimens, we cannot perform this direct measurement, which is potentially an important factor in post-insertional inflammatory response and subsequent new bone formation. Third, while radiologic studies such as Avci *et al.* are limited by decreased discernability of tissue planes and of the basilar membrane in particular, the utilization of histologic specimens is also subject to error, including those related to HTB processing, variations in H&E staining, as well as artifacts related to compression, folding, or mounting in general. However, improved discernability of the basilar membrane and boundaries of the scala tympani allow for accurate 3-D reconstruction and measurement of the dimensions of the scala tympani. Finally, the angular depth of insertion for each electrode, particularly for the detailed analysis of the CI632, CI622, and FLEX28 electrodes, are estimated using data from prior studies on the outer and inner cochlear wall lengths; these estimates may not reflect or account for variability during actual electrode insertion during surgery.

Conclusion

Utilizing 3-D reconstruction of histologic sections of human temporal bone specimens, the present study details the cross-sectional area of the scala tympani throughout the cochlea, as well as the vertical height of the scala tympani at the lateral wall, central, and perimodiolar horizontal locations. The cross-sectional dimensions of ten commonly used cochlear implant electrodes were evaluated and measured relative to the respective dimensions of the scala tympani, yielding a wide variability of ratio of space of the scala tympani occupied by the electrode and proximity of electrode to the basilar membrane. The potential implications in postoperative outcomes is explored. There were significant interval decreases in all three height measurements in the first 180° and from 450° to 540°; we also report a significant decrease in the mean lateral height relative to the perimodiolar height after 360°. The scala tympani shape changed from elliptical to a scalene triangular shape with the narrow tail at the perimodiolar end after 360°. These measurements provide potential explanation regarding the mechanism by which electrode translocation occurs with higher frequency at approximately 180° and 400°. Additional investigation should be conducted into the impact of electrode dimensions as well as the role of different types of electrodes in insertional trauma.

Acknowledgements:

Supported by NIDCD grant U24 DC 015910-01 (AI)

References

1. Wilson BS, Dorman MF. Cochlear implants: a remarkable past and a brilliant future. Hear Res. Aug 2008;242(1-2):3–21. doi:10.1016/j.heares.2008.06.005 [PubMed: 18616994]
2. Babajanian EE, Patel NS, Gurgel RK. The Impact of Cochlear Implantation: Cognitive Function, Quality of Life, and Frailty in Older Adults. Semin Hear. Nov 2021;42(4):342–351. doi:10.1055/s-0041-1739367 [PubMed: 34912162]
3. Chen DS, Betz J, Yaffe K, et al. Association of hearing impairment with declines in physical functioning and the risk of disability in older adults. J Gerontol A Biol Sci Med Sci. May 2015;70(5):654–61. doi:10.1093/gerona/glu207 [PubMed: 25477427]
4. Gantz BJ, Turner CW. Combining acoustic and electrical hearing. Laryngoscope. Oct 2003;113(10):1726–30. doi:10.1097/00005537-200310000-00012 [PubMed: 14520097]
5. Turner CW, Gantz BJ, Vidal C, Behrens A, Henry BA. Speech recognition in noise for cochlear implant listeners: benefits of residual acoustic hearing. J Acoust Soc Am. Apr 2004;115(4):1729–35. doi:10.1121/1.1687425 [PubMed: 15101651]
6. Ishiyama A, Ishiyama G, Lopez IA, Linthicum FH Jr.Temporal Bone Histopathology of First-Generation Cochlear Implant Electrode Translocation. Otol Neurotol. Jul 2019;40(6):e581–e591. doi:10.1097/mao.0000000000002247 [PubMed: 31058752]
7. Li PM, Somdas MA, Eddington DK, Nadol JB Jr.Analysis of intracochlear new bone and fibrous tissue formation in human subjects with cochlear implants. Ann Otol Rhinol Laryngol. Oct 2007;116(10):731–8. doi:10.1177/000348940711601004 [PubMed: 17987778]
8. Fayad JN, Makarem AO, Linthicum FH Jr.Histopathologic assessment of fibrosis and new bone formation in implanted human temporal bones using 3D reconstruction. Otolaryngol Head Neck Surg. Aug 2009;141(2):247–52. doi:10.1016/j.otohns.2009.03.031 [PubMed: 19643260]
9. Morrel WG, Holder JT, Dawant BM, Noble JH, Labadie RF. Effect of Scala Tympani Height on Insertion Depth of Straight Cochlear Implant Electrodes. Otolaryngol Head Neck Surg. May 2020;162(5):718–724. doi:10.1177/0194599820904941 [PubMed: 32093543]
10. Biedron S, Prescher A, Ilgner J, Westhofen M. The internal dimensions of the cochlear scalae with special reference to cochlear electrode insertion trauma. Otol Neurotol. Jul 2010;31(5):731–7. doi:10.1097/MAO.0b013e3181d27b5e [PubMed: 20142798]
11. Avci E, Nauwelaers T, Lenarz T, Hamacher V, Kral A. Variations in microanatomy of the human cochlea. J Comp Neurol. Oct 1 2014;522(14):3245–61. doi:10.1002/cne.23594 [PubMed: 24668424]
12. Hatsushika S, Shepherd RK, Tong YC, Clark GM, Funasaka S. Dimensions of the scala tympani in the human and cat with reference to cochlear implants. Ann Otol Rhinol Laryngol. Nov 1990;99(11):871–6. doi:10.1177/000348949009901104 [PubMed: 2241011]
13. Wysocki J Dimensions of the human vestibular and tympanic scalae. Hear Res. Sep 1999;135(1-2):39–46. doi:10.1016/s0378-5955(99)00088-x [PubMed: 10491952]
14. Ketterer MC, Aschendorff A, Arndt S, et al. The influence of cochlear morphology on the final electrode array position. Eur Arch Otorhinolaryngol. Feb 2018;275(2):385–394. doi:10.1007/s00405-017-4842-y [PubMed: 29242990]
15. Schurzig D, Timm ME, Majdani O, Lenarz T, Rau TS. The Use of Clinically Measurable Cochlear Parameters in Cochlear Implant Surgery as Indicators for Size, Shape, and Orientation of the Scala Tympani. Ear Hear. July/Aug 2021;42(4):1034–1041. doi:10.1097/aud.0000000000000998 [PubMed: 33480625]
16. Danielian A, Ishiyama G, Lopez IA, Ishiyama A. Morphometric linear and angular measurements of the human cochlea in implant patients using 3-dimensional reconstruction. Hear Res. Feb 2020;386:107874. doi:10.1016/j.heares.2019.107874 [PubMed: 31893539]
17. Verbist BM, Skinner MW, Cohen LT, et al. Consensus panel on a cochlear coordinate system applicable in histologic, physiologic, and radiologic studies of the human cochlea. Otol Neurotol. Jul 2010;31(5):722–30. doi:10.1097/MAO.0b013e3181d279e0 [PubMed: 20147866]
18. Hodge SE, Ishiyama G, Lopez IA, Ishiyama A. Histopathologic Analysis of Temporal Bones With Otosclerosis Following Cochlear Implantation. Otol Neurotol. Dec 1 2021;42(10):1492–1498. doi:10.1097/mao.0000000000003327 [PubMed: 34607995]

19. Dhanasingh A, Jolly C. An overview of cochlear implant electrode array designs. Hear Res. Dec 2017;356:93–103. doi:10.1016/j.heares.2017.10.005 [PubMed: 29102129]

20. Castilho AM, Pauna HF, Fernandes FL, et al. HiFocus Helix™ electrode insertion: surgical approach. BMC Res Notes. Jul 15 2015;8:304. doi:10.1186/s13104-015-1267-9 [PubMed: 26174835]

21. Cochlear Implant Electrode Comparison. Accessed April 15, 2022. https://www.cochlearelectrodes.com/assets/downloads/FUN1142-Electrode-Comparison-Sheet.pdf.

22. Dhanasingh A The rationale for FLEX (cochlear implant) electrode with varying array lengths. World J Otorhinolaryngol Head Neck Surg. Jan 2021;7(1):45–53. doi:10.1016/j.wjorl.2019.12.003 [PubMed: 33474544]

23. Shakeel M, Spielmann PM, Jones SE, Hussain SS. Direct measurement of the round window niche dimensions using a 3-dimensional moulding technique--a human cadaveric temporal bone study. Clin Otolaryngol. Dec 2015;40(6):657–61. doi:10.1111/coa.12438 [PubMed: 25891637]

24. Dhanasingh A, Swords C, Bance M, Van Rompaey V, Van de Heyning P. Cochlear Size Assessment Predicts Scala Tympani Volume and Electrode Insertion Force- Implications in Robotic Assisted Cochlear Implant Surgery. Front Surg. 2021;8:723897. doi:10.3389/fsurg.2021.723897 [PubMed: 34660676]

25. Danielian A, Ishiyama G, Lopez IA, Ishiyama A. Predictors of Fibrotic and Bone Tissue Formation With 3-D Reconstructions of Post-implantation Human Temporal Bones. Otol Neurotol. Aug 1 2021;42(7):e942–e948. doi:10.1097/mao.0000000000003106 [PubMed: 33710156]

26. Kamakura T, Nadol JB Jr.Correlation between word recognition score and intracochlear new bone and fibrous tissue after cochlear implantation in the human. Hear Res. Sep 2016;339:132–41. doi:10.1016/j.heares.2016.06.015 [PubMed: 27371868]

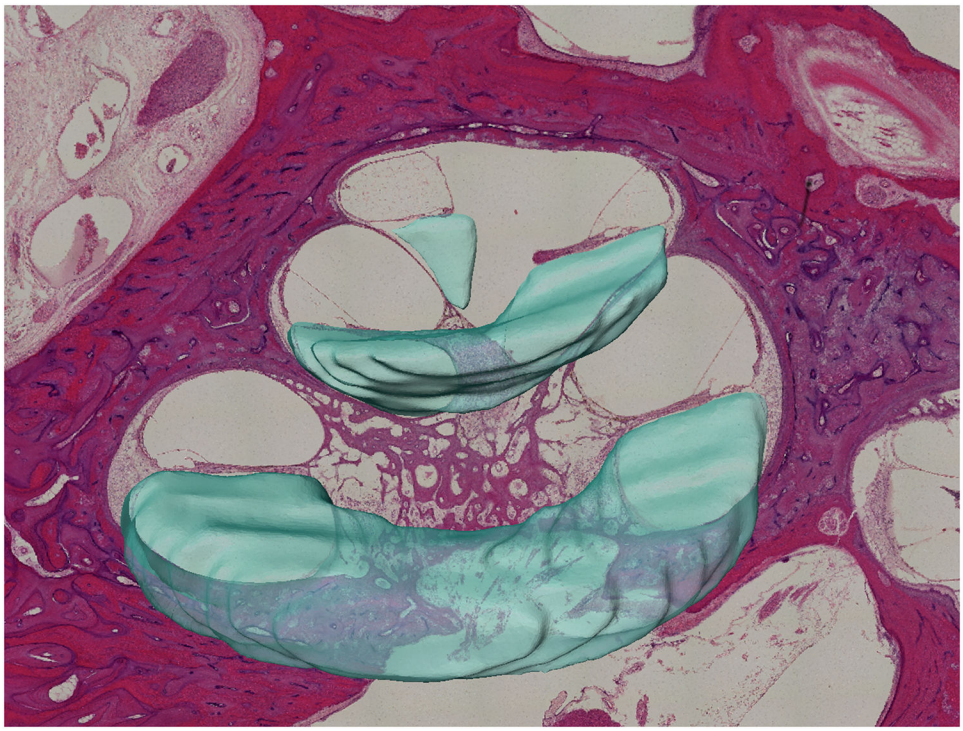

Figure 1.
Segmentation and 3-D reconstruction of scala tympani superimposed on mid-modiolar histologic section.

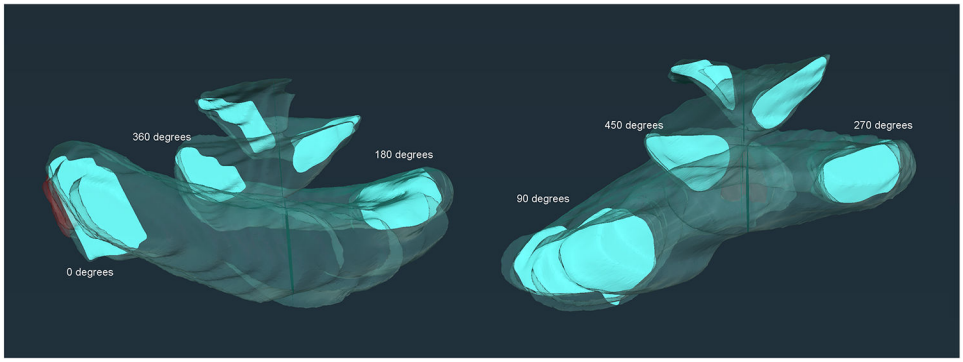

Figure 2.

Cross-sections of 3-D reconstruction of scala tympani for vertical height and cross-sectional area measurements every 90°. Once segmentation and surface generation of the scala tympani was complete, cross-sections were generated every 90° and separately analyzed using linear measurement tools.

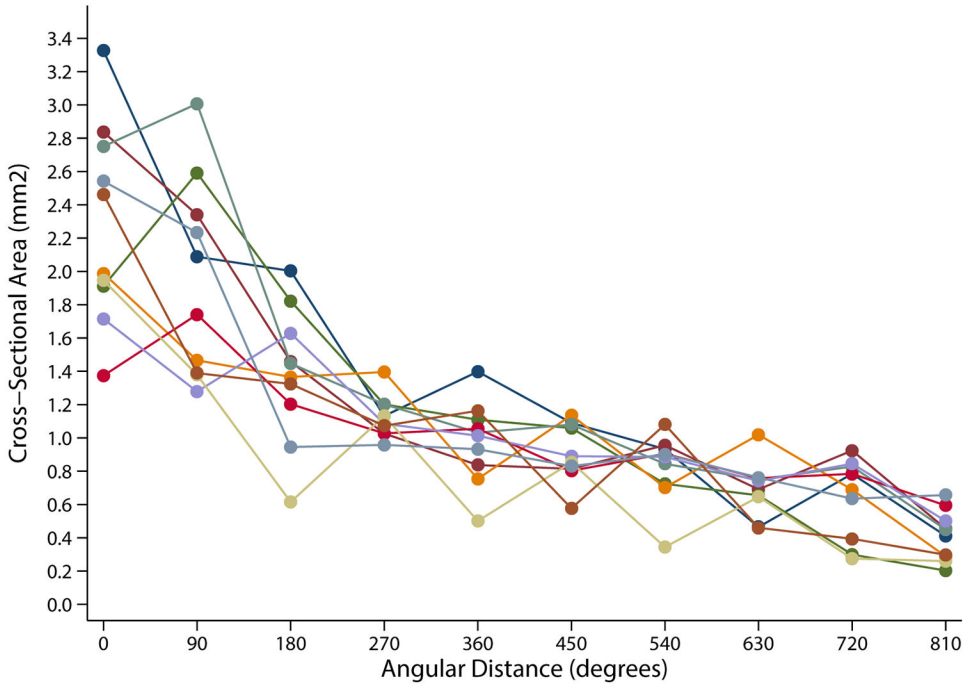

Figure 3.

Cross-sectional area (mm^2) of the scala tympani as a function of angular distance in 10 human temporal bone specimens. The cross-sectional area was measured in 90° intervals and significant decreased from 2.29 mm^2 (sd 0.60) to 1.38 mm^2 (sd 0.13) from 0° to 180° (p=0.001).

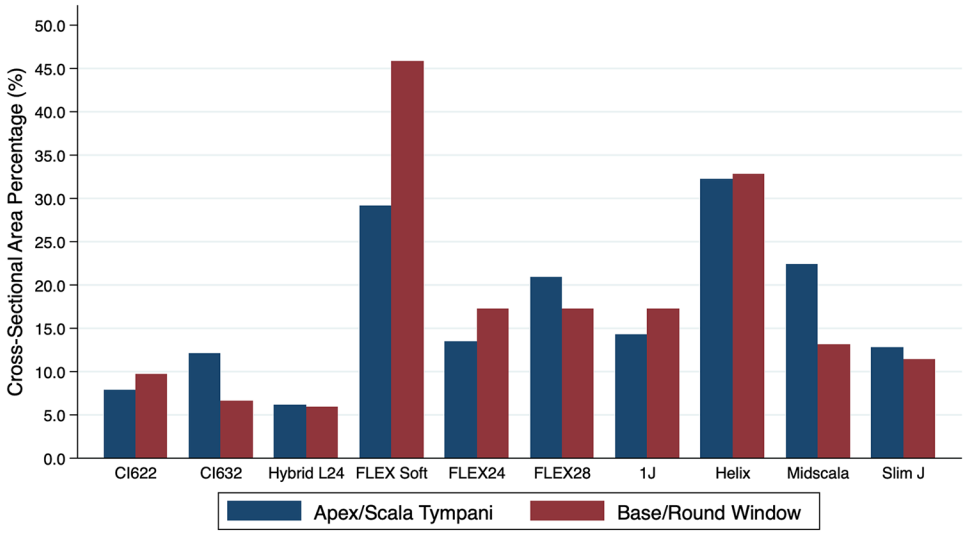

Figure 4.

Percentage of scala tympani and round window cross-sectional area occupied by cochlear implant electrodes at full insertion. The insertion depth angle was obtained from Dhanasingh and Jolly in 2017. Measurements of the round window area were determined by Shakeel *et al.* in 2015.

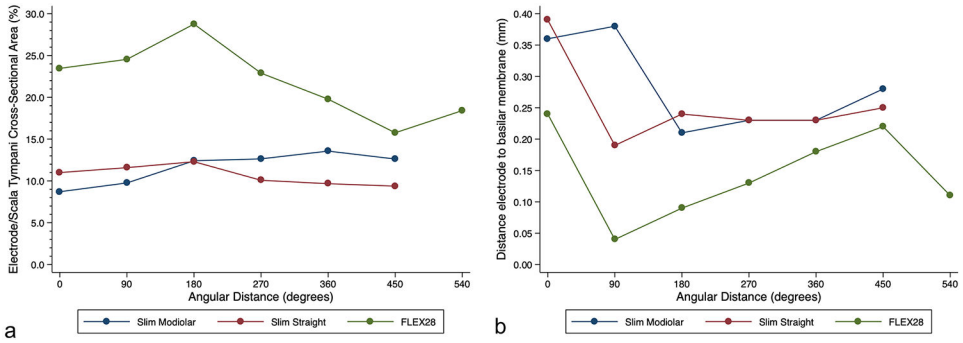

Figure 5.

Detailed cross-sectional area (a) and vertical distance from basilar membrane (b) measurements for CI632, CI622, and FLEX 28 electrodes. Measurements were recorded at 90° intervals for all three electrodes. When comparing the lateral wall electrodes, the CI622 occupied a mean 10.67% (sd 3.24%) of cross-sectional area, compared to 21.94% (sd 7.90%) for the FLEX 28 electrode.

Table 1.

Means and standard deviations of central, lateral, and perimodiolar height measurements of the scala tympani.

Angular distance (°)	Central height, mm (SD)	Lateral height, mm (SD)	Perimodiolar height, mm (SD)
0	1.79 (0.38)	1.28 (0.25)	1.20 (0.29)
90	1.39 (0.14)	0.85 (0.10)	1.21 (0.35)
180	1.09 (0.15)	0.88 (0.14)	0.85 (0.15)
270	0.99 (0.16)	0.81 (0.17)	0.86 (0.11)
360	1.01 (0.18)	0.78 (0.17)	0.83 (0.23)
450	1.01 (0.10)	0.79 (0.20)	0.91 (0.24)
540	0.81 (0.15)	0.59 (0.11)	0.73 (0.19)
630	0.72 (0.11)	0.53 (0.13)	0.71 (0.14)
720	0.60 (0.18)	0.39 (0.18)	0.66 (0.25)
810	0.46 (0.13)	0.34 (0.13)	0.53 (0.21)